

Magnetic birefringence of light in the antiferromagnetic MnCO_3 , CoCO_3 , and CsMnF_3

A. S. Borovik-Romanov, N. M. Kreines, A. A. Pankov, and M. A. Talalaev

Institute of Physics Problems, USSR Academy of Sciences

(Submitted September 18, 1973)

Zh. Eksp. Teor. Fiz. **66**, 782-791 (February 1974)

The temperature dependence of the birefringence of light was investigated in the rhombohedral MnCO_3 and CoCO_3 and in the hexagonal CsMnF_3 . It was observed that the difference $\Delta n = n_{\perp} - n_{\parallel}$ in these compounds experiences a strong change in the region of the corresponding Néel points. The MnCO_3 and CsMnF_3 remain optically uniaxial crystals, regardless of the orientation of the antiferromagnetism vector \mathbf{l} in the basal plane. A dependence of the refractive-index difference on the direction of \mathbf{l} is observed in CoCO_3 , and this crystal becomes optically biaxial in the single-domain state. The results are discussed on the basis of the phenomenological expression for the tensor ϵ_{ij} of the compounds in question.

INTRODUCTION

In earlier papers^[1,2] we reported investigations of the influence of magnetic ordering on the birefringence of light in the antiferromagnetic crystals MnF_2 , CoF_2 , and NiF_2 . In the present paper we report similar investigations on antiferromagnets with a different magnetic structure, MnCO_3 , CoCO_3 , and CsMnF_3 .

The study of birefringence of a number of magnetically-ordered crystals (iron garnets^[3-5] and antiferromagnets^[6-8,1,2]) shows that the transition to the ordered state is accompanied by an abrupt change in the difference between the refractive indices of the crystals. We have shown^[1,2] that the sign and magnitude of this effect in MnF_2 , CoF_2 , and NiF_2 cannot be attributed to the change produced by spontaneous striction in the lattice constants of the crystal. It appears that there is another not so trivial mechanism whereby the magnetically ordered state influences the birefringence. This magnetic contribution Δn_{mag} can be separated from the experimentally-measured difference between the refractive indices, as is done in^[2], if the temperature dependence of the crystal lattice constants is known at sufficiently wide temperature intervals.

A study of the dependence of Δn_{mag} on the magnetic structure of matter shows that in MnF_2 and NiF_2 the value of Δn_{mag} is independent of the direction of the antiferromagnetism vector \mathbf{l} relative to the crystallographic axes and the direction of the propagation of the light. In CoF_2 , in addition to this isotropic Δn_{mag} , there is observed an anisotropic increment of Δn_{mag} , which depends on the components l_i . We note that by measuring the refractive-index differences it is possible to observe the isotropic effect only in crystals with symmetries lower than cubic.

The study of birefringence in MnCO_3 , CoCO_3 , and CsMnF_3 is of interest, in particular, because they are easy-plane antiferromagnets, unlike the uniaxial MnCO_3 , CoF_2 , and NiF_2 , in which the anisotropy in the plane is appreciable.

SAMPLES AND PROCEDURE

In the paramagnetic state, MnCO_3 , CoCO_3 , and CsMnF_3 are optically uniaxial crystals. The crystallographic symmetry of the isomorphous MnCO_3 and CoCO_3 is described by the symmetry group \tilde{D}_{3d}^6 , while the symmetry of CsMnF_3 is described by \tilde{D}_{6h}^4 . The unit

cell of MnCO_3 or CoCO_3 contains two magnetic ions^[9], while that of CsMnF_3 contains six Mn^{2+} ions occupying two non-equivalent positions^[10]. When the temperature is lowered, these compounds go over into an ordered antiferromagnetic state of the easy-plane type. The magnetic vectors of the sublattices in MnCO_3 and CoCO_3 are then canted and form a spontaneous magnetic vector \mathbf{m} , which lies in the basal plane and is perpendicular to the antiferromagnetic vector \mathbf{l} . The value of m is approximately 0.2% in MnCO_3 and approximately 5% of the nominal value of the sublattice magnetization in CoCO_3 . According to the data of Alikhanov^[11], in the absence of an external magnetic field the vector \mathbf{l} in CoCO_3 lies in the vertical symmetry plane at an angle $\sim 45^\circ$ to the threefold axis C_3 . The compound CsMnF_3 is a pure antiferromagnet^[12].

In the basal plane, the crystallographic anisotropy of all three compounds is low, and therefore in a magnetic field (0.5–2 kOe), regardless of the field direction, the vector \mathbf{l} always becomes perpendicular to the field in this plane, and the vector \mathbf{m} , if it exists, is oriented along the field.

Certain magnetic and optical characteristics of the investigated substance are listed in the table. We know of no data whatever concerning the refractive indices of CsMnF_3 .

The MnCO_3 and CoCO_3 crystals were grown at the Crystallography Institute of the USSR Academy of Sciences. The CsMnF_3 was grown by S. V. Petrov of our Institute^[1]. The selected crystals were x-ray oriented and cut in the form of rectangular parallelepipeds. The edges of the MnCO_3 and CoCO_3 parallelepipeds coincided with the directions of C_3 (the z axis) and C_2 (the x axis), with $y \perp x \perp z$; in CsMnF_3 they coincided with the directions of C_6 (z axis) and C_2 (x axis), with $y \perp x \perp z$.

We measured the dependences of the refractive-

Compound	$T_N, ^\circ\text{K}$	H_E, kOe	H_D, kOe	$\chi_1 \cdot 10^3, \text{emu/mole}$	$n_o (T=300^\circ\text{K})$	$n_e (T=300^\circ\text{K})$
MnCO_3	29.0	32.4 *	320	4.4	43	1.816
CoCO_3	47.0	18.1 *	460	27	52	1.855
CsMnF_3		53.5 *	350	—	39.7	—

*The values of T_N marked by an asterisk were obtained from magnetic measurements, and those without an asterisk were obtained by Kalinkina^[14] from the measurements of the specific heat C_p of MnCO_3 and CoCO_3 .

index difference Δn on the temperature and on the magnetic field. The refractive-index difference Δn was measured with apparatus described in [2] by a method with direct compensation for the path difference. The accuracy with which Δn was measured depended on the quality of the crystal and ranged from 5×10^{-6} to 2×10^{-5} . The sample was placed in an evacuated cell in an optical cryostat. The sample temperature was measured with a ZLZh-99-chromel thermocouple. The relative temperature-measurement accuracy was $\pm 0.05^\circ$, and the absolute accuracy was $\pm 0.3^\circ$. In a number of experiments, if no magnetic field was required, the single vacuum cell was replaced by a double cell constructed to resemble a Dewar. The jacket of this cell was evacuated to $\sim 10^{-3}$ mm Hg, and the internal part was filled with helium gas (~ 1 mm Hg). This construction improved the thermal contact between the sample and the cold junction of the thermocouple and kept the sample from sticking.

The magnetic field was produced with a superconducting solenoid and reached ~ 50 kOe.

EXPERIMENTAL RESULTS

MnCO₃

Just as in [2], the difference of the refractive indices was measured at two experimental configurations. In the first configuration light propagated in MnCO₃ along the y axis, and the polarization plane made an angle 45° to the x and z axis. In this geometry we determined the temperature dependence of the refractive-index difference for light waves polarized along the x and z axes. A plot of $\Delta n_{xz}(T) = (n_x - n_z)T - (n_x - n_z)300^\circ\text{K}$ is shown in Fig. 1. We see that in the region of 30°K there is an abrupt decrease of $\Delta n_{xz}(T)$. On the whole, the curve resembles the analogous plot for MnF₂. The Néel point was determined from the maximum of the derivative $d(\Delta n_{xz})/dT$ and amounted to 32°K . No kink could be observed on the $\Delta n_{xz}(T)$ curve at the point T_N , apparently because of the insufficient measurement accuracy. The value $T_N = 32^\circ\text{K}$ differs from the value $T_N = 29.5^\circ\text{K}$ obtained in measurements of the temperature dependence of the specific heat c_p in MnCO₃ [14], but agrees quite well with magnetic-measurement data [13] ($T_N = 32.4^\circ\text{K}$). According to the latter, turning on a magnetic field in the basal plane orients the magnetic domains in this plane. In our experiments, the field was directed along the x axis, and consequently

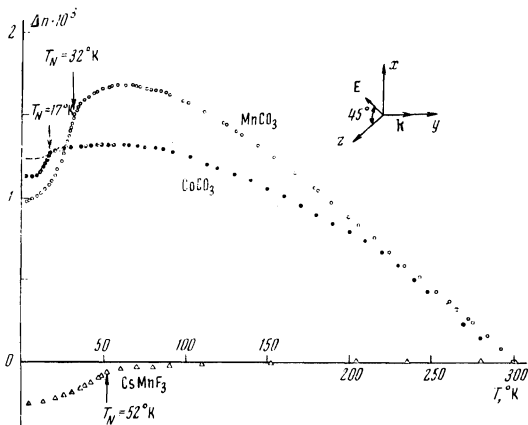


FIG. 1. Temperature dependence of the difference between the refractive indices Δn_{xz} in MnCO₃, CoCO₃, CsMnF₃. The points below T_N of CoCO₃ show the variation of Δn_{xz} in a magnetic field 2 kOe, while the dashed curve shows the variation of Δn_{xz} in the absence of a magnetic field.

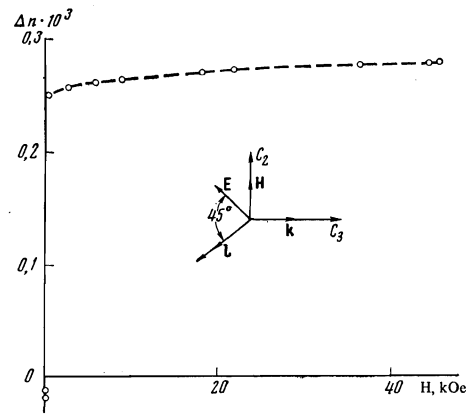


FIG. 2. Dependence of the refractive-index difference Δn_{yx} in CoCO₃ on the magnetic field applied along the x axis; $T = 3.0^\circ\text{K}$.

the vector l oriented itself along the y axis. Within the limits of the experimental accuracy, we observed no change of $\Delta n_{xz}(T)$ whatever at any temperature and in magnetic fields up to 50 kOe.

A similar lack of change in the refractive indices when the domains become oriented by the field was observed also in the second experimental configurations, when the light propagated along the z axis. The difference $\Delta n_{xy}(T) = n_x - n_y$ turn out to be zero at all temperatures and fields. It follows from the results of the experiments with the magnetic field that the magnetic birefringence in MnCO₃, just as in MnF₂, does not depend on the direction of the vector l relative to the crystallographic axes.

CoCO₃

The experiments with CoCO₃ were performed on two different samples, since the poor quality and small dimensions of the crystals at our disposal did not make it possible to prepare a sample that was sufficiently transparent simultaneously in two perpendicular directions. In the field experiment the light was directed along the z axis and we measured the refractive-index difference for waves polarized along the x and y axes. In the absence of a magnetic field, the difference $\Delta n_{yx} = n_y - n_x$ is not single-valued and does not exceed $\sim 10^{-5}$. In magnetic fields corresponding to orientation of the magnetic domains, the difference Δn_{yx} increases sharply—see Fig. 2 (the curve in Fig. 2 was obtained at a sample temperature 3.0°K). This change of Δn_{yx} in the course of magnetization of the sample was first observed in CoCO₃ by Kharchenko et al. [15] by the method of conoscopic figures. As follows from Fig. 2, the difference Δn_{yx} continues to increase in magnetic fields greatly exceeding the value at which the domains become oriented in the crystal.

The temperature dependence of Δn_{yx} at certain values of the magnetic field is shown in Fig. 3. The same figure shows for comparison data from [15], and also the temperature dependence of the square of the weak ferromagnetic vector m [13]. The $m^2(T)$ curve can be successfully aligned with the $\Delta n_{yx}(T)$ curves obtained in strong magnetic fields. Our measurements of $\Delta n_{yx}(T)$ in weak fields yield a transition temperature $T_N = 17.0^\circ\text{K}$, which agrees with the measurements of the specific heat c_p of CoCO₃ [14]. Magnetic measurements yield $T_N = 18.1^\circ\text{K}$. When the magnetic field is increased, the different Δn_{yx} does not vanish at 17°K . This dragging of the curves at high temperatures seems to be

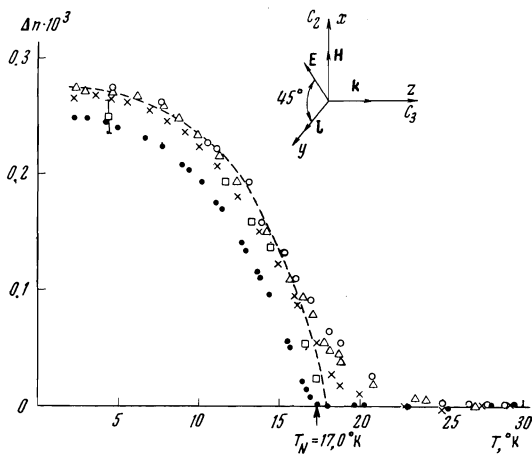


FIG. 3. Temperature dependence of the refractive-index difference Δn_{yx} in CoCO_3 , obtained in various magnetic fields: \bullet — $H = 1.8$ kOe, \times — $H = 18.5$ kOe, Δ — $H = 37$ kOe, \circ — $H = 46$ kOe, \square —data of [15]. The dashed curves show the temperature of the square of the weak ferromagnetic vector $\sigma^2(T)$.

connected with the antiferromagnetism induced by the magnetic field^[13].

In the other experimental geometry, the light was directed along the y axis and the temperature dependence of the refractive-index difference was measured for light waves polarized along the x and z axes

$$\Delta n_{xz}(T) = (n_x - n_z)_T - (n_x - n_z)_{3000^\circ\text{K}}$$

Without the external magnetic field, the change $\Delta n_{xz}(T)$ as a result of the magnetic ordering is small, about 0.3×10^{-4} . In Fig. 1, the plot of $\Delta n_{xz}(T)$ below T_N is shown dashed.

Just as in the preceding experimental configuration, the orientation of the domains by the magnetic field causes an abrupt change of $\Delta n_{xz}(T)$ below the transition point (see Fig. 1). A field ~ 2 kOe was applied in this experiment along the x axis, and the vector l , as is well known, oriented itself in a plane perpendicular to the field.

A kink is observed on the $\Delta n_{xz}(T)$ curves plotted without and with a field. Its position at 17°K coincides with the value obtained in the first experiment with this compound (see Fig. 3). The maximum change of $\Delta n_{xz}(T)$ following application of a magnetic field (~ 2 kOe) is

$$\Delta n_{xz}(T) = (n_x - n_z)_H - (n_x - n_z)_{H=0} \approx 1.3 \cdot 10^{-4}. \quad (1)$$

Unlike the preceding configuration, this quantity remained constant, within the limits of experimental accuracy, when the field was increased to ~ 50 kOe. Thus, the birefringence in CoCO_3 , as in CoF_2 , turns out to depend on the orientation of the vector l relative to the crystallographic axes.

CsMnF₃

The temperature dependence of the refractive-index difference in CsMnF_3 duplicates qualitatively the results obtained earlier for MnF_2 ^[2] and in the present study for MnCO_3 . The crystal remains optically uniaxial at all temperatures and magnetic fields applied in the region T_N and does not depend on the applied field. The plot of

$$\Delta n_{xz}(T) = (n_x - n_z)_T - (n_x - n_z)_{3000^\circ\text{K}}$$

is shown in Fig. 1. The obtained value $T_N = 52^\circ\text{K}$ differs somewhat from the 53.5°K known from magnetic measurements.

To separate Δn_{mag} for MnCO_3 , CoCO_3 and CsMnF_3 , as was done in^[2] for MnF_2 and CoF_2 , data are necessary on the temperature dependence of the lattice constants of the investigated compounds. Unfortunately, no such data are known to us.

THE DIELECTRIC TENSOR ϵ_{ij}

The dependence of the refractive indices of the components of the tensor ϵ_{ij} on the magnetic state of the crystal can be described by starting from symmetry considerations, as was done in^[2]. The components of the tensor ϵ_{ij} are obtained from the expression for the density of the internal electromagnetic energy of light in a crystal, with allowance for the terms quadratic in the magnetic moments, which are responsible for the magnetic birefringence. We assume here that in antiferromagnets the magnetic birefringence is determined primarily by the vector l , inasmuch as the value of the vector m is always much lower.

For MnCO_3 and CoCO_3 , taking into account the symmetry of the crystal (symmetry group \tilde{D}_{3d}^6), the expression for the electromagnetic-energy density is

$$\begin{aligned} \mathcal{E} = \mathcal{E}_0 + \frac{1}{8\pi} \{ & \lambda_1 E_x^2 l^2 + \lambda_2 (E_x^2 + E_y^2) l^2 + \lambda_3 E_x^2 l_z^2 + \lambda_4 (E_x^2 + E_y^2) l_z^2 \\ & + \lambda_5 E_x l_x (E_x l_x + E_y l_y) + \lambda_6 E_x [E_y (l_x^2 - l_y^2) + E_x 2l_x l_y] + \lambda_7 l_z [(E_x^2 - E_y^2) l_y \\ & + 2E_x E_y l_x] + \lambda_8 [(E_x^2 - E_y^2) (l_x^2 - l_y^2) + 4E_x E_y l_x l_y] \}. \end{aligned} \quad (2)$$

The second derivatives of \mathcal{E} with respect to E_i and E_j are the components of the tensor ϵ_{ij} :

$$\begin{aligned} \epsilon_{xx} &= \epsilon_{\perp}^0 + 2\lambda_1 l^2 + 2\lambda_2 l_z^2 + 2\lambda_4 l_x l_y + 2\lambda_8 (l_x^2 - l_y^2), \\ \epsilon_{yy} &= \epsilon_{\perp}^0 + 2\lambda_2 l^2 + 2\lambda_1 l_z^2 - 2\lambda_4 l_x l_y - 2\lambda_8 (l_x^2 - l_y^2) \\ \epsilon_{zz} &= \epsilon_{\parallel}^0 + 2\lambda_3 l^2 + 2\lambda_5 l_z^2, \quad \epsilon_{xy} = \epsilon_{yx} = \lambda_7 l_x l_z + 2\lambda_6 l_x l_y, \\ \epsilon_{xz} &= \epsilon_{zx} = \frac{1}{2} \lambda_5 l_x l_z + \lambda_6 l_x l_y, \\ \epsilon_{yz} &= \epsilon_{zy} = \frac{1}{2} \lambda_5 l_x l_y + \frac{1}{2} \lambda_6 (l_x^2 - l_y^2). \end{aligned} \quad (3)$$

Here ϵ_{\perp}^0 and ϵ_{\parallel}^0 are the diagonal elements of the tensor ϵ_{ij} for the uniaxial crystals MnCO_3 and CoCO_3 in the paramagnetic state.

Unlike the two-sublattice antiferromagnets MnCO_3 and CoCO_3 , the compound CsMnF_3 is a six-sublattice antiferromagnet and \mathcal{E} should be resolved along the vectors^[16]

$$\begin{aligned} l_1 &= s_1 - s_2, & m_1 &= s_1 + s_2; \\ l_2 &= -\sigma_1 + \sigma_2 + \sigma_3 - \sigma_4, & l_3 &= -\sigma_1 - \sigma_2 + \sigma_3 + \sigma_4, \\ l_4 &= -\sigma_1 + \sigma_2 - \sigma_3 + \sigma_4, & m_2 &= \sigma_1 + \sigma_2 + \sigma_3 + \sigma_4. \end{aligned}$$

Here s_1 and s_2 are the magnetic moments of the Mn II ions occupying the crystallographic positions $(0, 0, 0)$ and $(0, 0, \frac{1}{2})$; $\sigma_1, \sigma_2, \sigma_3$, and σ_4 are the magnetic moments of the ions Mn II occupying the positions $(\frac{1}{3}, \frac{2}{3}, u)$, $(\frac{1}{3}, \frac{2}{3}, \frac{1}{2} - u)$, $(\frac{2}{3}, \frac{1}{3}, \frac{1}{3} + u)$ and $(\frac{2}{3}, \frac{1}{3}, -u)$. However, inasmuch as the vectors m_1, m_2, l_3 , and l_4 are much smaller than l_1 and l_2 , we confine ourselves in the expansion to terms quadratic in l_1 and l_2 :

$$\begin{aligned} \mathcal{E} = \mathcal{E}_0 + \frac{1}{8\pi} \{ & \alpha_1 E_x^2 l_1^2 + \beta_1 E_x^2 l_2^2 + \gamma_1 E_x^2 l_1 l_2 + \alpha_2 (E_x^2 + E_y^2) l_1^2 + \beta_2 (E_x^2 + E_y^2) l_2^2 \\ & + \gamma_2 (E_x^2 + E_y^2) l_1 l_2 + \alpha_3 E_x^2 l_1^2 + \beta_3 E_x^2 l_2^2 + \gamma_3 E_x^2 l_1 l_2 + \alpha_4 (E_x^2 + E_y^2) l_1^2 \\ & + \beta_4 (E_x^2 + E_y^2) l_2^2 + \gamma_4 (E_x^2 + E_y^2) l_1 l_2 + \alpha_5 E_x l_{1x} (E_x l_{1x} + E_y l_{1y}) \\ & + \beta_5 E_x l_{2x} (E_x l_{2x} + E_y l_{2y}) + \gamma_5 E_x l_{1z} (E_x l_{2x} + E_y l_{2y}) + \eta_5 E_x^2 s_{2z} (E_x l_{1x} + E_y l_{1y}) \\ & + \alpha_6 [(E_x^2 - E_y^2) (l_{1x}^2 - l_{1y}^2) + 4E_x E_y l_{1x} l_{1y}] + \beta_6 [(E_x^2 - E_y^2) (l_{2x}^2 - l_{2y}^2) \\ & + 4E_x E_y l_{2x} l_{2y}] + \gamma_6 [(E_x^2 - E_y^2) (l_{1x} l_{2x} - l_{1y} l_{2y}) + 2E_x E_y (l_{1x} l_{2y} + l_{2x} l_{1y}) \}. \end{aligned} \quad (4)$$

Here $\alpha_i, \beta_i, \gamma_i$, and η_i are the magneto-optical constants.

The components of the tensor ϵ_{ij} for CsMnF_3 are given by

$$\begin{aligned}
\varepsilon_{xx} &= \varepsilon_{\perp}^0 + 2\alpha_2 l_x^2 + 2\beta_2 l_y^2 + 2\gamma_2 l_z^2 + 2\alpha_4 l_x l_y + 2\beta_4 l_x l_z + 2\gamma_4 l_y l_z, \\
\varepsilon_{yy} &= \varepsilon_{\perp}^0 + 2\alpha_2 l_x^2 + 2\beta_2 l_y^2 + 2\gamma_2 l_z^2 + 2\alpha_4 l_x l_y + 2\beta_4 l_x l_z + 2\gamma_4 l_y l_z, \\
\varepsilon_{zz} &= \varepsilon_{\parallel}^0 + 2\alpha_1 l_x^2 + 2\beta_1 l_y^2 + 2\gamma_1 l_z^2 + 2\alpha_3 l_x l_y + 2\beta_3 l_x l_z + 2\gamma_3 l_y l_z, \\
\varepsilon_{xy} &= \varepsilon_{yx} = 2\alpha_4 l_x l_y + 2\beta_4 l_x l_z + 2\gamma_4 l_y l_z, \\
\varepsilon_{xz} &= \varepsilon_{zx} = 1/2 \alpha_3 l_x l_z + 1/2 \beta_3 l_x l_z + 1/2 \gamma_3 l_x l_z, \\
\varepsilon_{yz} &= \varepsilon_{zy} = 1/2 \alpha_3 l_y l_z + 1/2 \beta_3 l_y l_z + 1/2 \gamma_3 l_y l_z.
\end{aligned} \quad (5)$$

Experiments have yielded for MnCO_3 and CsMnF_3 the following: a) Δn_{xy} is equal to zero also in the magnetically-ordered region, both in a zero magnetic field and in fields up to ~ 50 kOe, b) Δn_{xz} does not vary under the influence of the orientation by the field of the vector l . Therefore the anisotropic terms in the tensor ε_{ij} should be regarded as small. The difference between the principal refractive indices for these crystals takes the following form: for MnCO_3

$$\Delta n_{xz} = n_{\perp}^0 - n_{\parallel}^0 + l^2 \left(\frac{\lambda_2}{n_{\perp}^0} - \frac{\lambda_1}{n_{\parallel}^0} \right) \quad (6)$$

and for CsMnF_3

$$\Delta n_{xz} = n_{\perp}^0 + n_{\parallel}^0 + l^2 \left(\frac{\alpha_2}{n_{\perp}^0} - \frac{\alpha_1}{n_{\parallel}^0} \right) + l_z^2 \left(\frac{\beta_2}{n_{\perp}^0} - \frac{\beta_1}{n_{\parallel}^0} \right) + l_x l_z \left(\frac{\gamma_2}{n_{\perp}^0} - \frac{\gamma_1}{n_{\parallel}^0} \right), \quad (7)$$

where $n_{\perp}^0 = (\varepsilon_{\perp}^0)^{1/2}$ and $n_{\parallel}^0 = (\varepsilon_{\parallel}^0)^{1/2}$.

Inasmuch as a dependence of the refractive indices on the direction of the vector l appears in CoCO_3 , just as in CoF_2 , it is necessary to take into account the anisotropic terms of the tensor ε_{ij} of this compound. In a zero magnetic field, as is well known^[15,17], the crystal is broken up into domains that are parallel to the base plane, with the angles between their vectors l not equal to 180° . In this case the ε_{ij} terms proportional to the products of different components of the vector l and to the expression $l_x^2 - l_y^2$ make no contribution to the refractive-index difference after averaging over the volume of the crystal. In this state, CoCO_3 should behave like an optically uniaxial crystal, and the difference between the refractive indices for the ordinary and extraordinary rays takes the form

$$\Delta n_{xz}^{\text{H=0}} = n_{\perp}^0 - n_{\parallel}^0 + l^2 \left(\frac{\lambda_2}{n_{\perp}^0} - \frac{\lambda_1}{n_{\parallel}^0} \right) + l_z^2 \left(\frac{\lambda_4}{n_{\perp}^0} - \frac{\lambda_3}{n_{\parallel}^0} \right). \quad (8)$$

As already noted, the change of the quantity $\Delta n_{xz}^{\text{H=0}}$ in antiferromagnetic ordering is small (see Fig. 1). This situation is reminiscent of the behavior of the difference Δn_{xz} in CoF_2 ^[2]. In the latter compound, the spontaneous striction is anomalously large, and therefore the change in the difference between the refractive indices Δn_{xz} lat, due to the striction, is larger than Δn_{xz} mag. This causes the experimentally measured refractive-index difference, which is the sum of these two effects of opposite sign, to be smaller than Δn_{xz} mag and to be opposite to it in sign. By analogy it can be assumed that Δn_{xz} lat, practically cancels out Δn_{xz} mag in CoCO_3 .

In a magnetic field directed along the x axis, the component l_x turns out to be small and those ε_{ij} terms which contain l_x can be neglected. We then obtain for CoCO_3

$$\begin{aligned}
\varepsilon_{xx} &= \varepsilon_{\perp}^0 + 2\lambda_2 l^2 + 2\lambda_4 l_x^2 + 2\lambda_7 l_x l_y - 2\lambda_8 l_y^2, \\
\varepsilon_{yy} &= \varepsilon_{\perp}^0 + 2\lambda_2 l^2 + 2\lambda_4 l_x^2 - 2\lambda_7 l_x l_y + 2\lambda_8 l_y^2, \\
\varepsilon_{zz} &= \varepsilon_{\parallel}^0 + 2\lambda_1 l^2 + 2\lambda_3 l_z^2, \quad \varepsilon_{xy} = \varepsilon_{yx} = \varepsilon_{xz} = \varepsilon_{zx} = 0, \\
\varepsilon_{yz} &= \varepsilon_{zy} = 1/2 \lambda_5 l_x l_z - 1/2 \lambda_6 l_y l_z.
\end{aligned} \quad (9)$$

In this state the crystal becomes biaxial, as is observed in the experiment. The tensor ε_{ij} is diagonalized when the y and z axes are rotated about the x axis through an angle α :

$$\text{tg } 2\alpha = \frac{\lambda_5 l_x l_y}{\varepsilon_{\parallel}^0 - \varepsilon_{\perp}^0} - \frac{\lambda_6 l_y^2}{\varepsilon_{\parallel}^0 - \varepsilon_{\perp}^0}. \quad (10)$$

Since α is proportional to the ratios $\lambda_5/(\varepsilon_{\parallel}^0 - \varepsilon_{\perp}^0)$ and $\lambda_6/(\varepsilon_{\parallel}^0 - \varepsilon_{\perp}^0)$, this angle is small. And since this rotation changes the component of the tensor ε_{ij} by amounts proportional to the squares of these ratios, the entire subsequent calculation was carried out for the initial coordinate system.

If the light is incident along the z axis and the field is applied, as before, along the x axis, then

$$\Delta n_{yx} = \frac{2\lambda_8}{n_{\perp}^0} l_y^2 - \frac{2\lambda_7}{n_{\perp}^0} l_x l_y. \quad (11)$$

This difference, as follows from Fig. 2, continues to increase at magnetic-field values greatly exceeding the value at which the domains are oriented in the crystal. If this growth were to be connected with additional orientation of the domains pinned by crystal defects, then the $\Delta n_{yx}(T)$ curves of Fig. 3, corresponding to different fields, would come closer together with increasing temperature, whereas the difference between them increases starting with low temperatures.

One of the possible explanations of the growth of Δn_{yz} in strong magnetic fields is connected with the effect observed by Bazhan^[18] in NiCO_3 . As is well known from neutron-diffraction measurements^[11,19], in the isomorphic NiCO_3 and CoCO_3 the vector l , in the absence of an external magnetic field, lies in a vertical symmetry plane and makes angles $\sim 22^\circ$ and 45° with the basal plane, respectively. As shown by Bazhan, in NiCO_3 this angle is a function of the crystal temperature and of the field applied in the basal plane, and vanishes at a critical field value 14 kOe. If we assume a similar effect in CoCO_3 , then the projections l_z and l_y vary with a field parallel to the x axis, and therefore the difference Δn_{yx} should depend on the field also after the vanishing of the domain structure.

In the other configuration ($\mathbf{k}_{\text{light}} \parallel y$, $\mathbf{H} \parallel x$), the orientation of the domains by the field causes the difference Δn_{xz} to take the form

$$\Delta n_{xz}^{\text{H}\parallel x} = n_{\perp}^0 - n_{\parallel}^0 + l^2 \left(\frac{\lambda_2}{n_{\perp}^0} - \frac{\lambda_1}{n_{\parallel}^0} \right) + l_z^2 \left(\frac{\lambda_4}{n_{\perp}^0} - \frac{\lambda_3}{n_{\parallel}^0} \right) + \frac{\lambda_7}{n_{\perp}^0} l_x l_y - \frac{\lambda_8}{n_{\perp}^0} l_y^2. \quad (12)$$

In Fig. 1, the plot of $\Delta n_{xz}^{\text{H=0}}$ is shown dashed. The values of $\Delta n_{xz}^{\text{H=0}}$ are marked by points. The change of $\Delta n_{xz}(T)$ as the domain structure vanishes is observed only in the antiferromagnetic region.

In conclusion, we thank P. L. Kapitza for interest in the work and I. E. Dzyaloshinskii for useful discussions.

APPENDIX

In our earlier paper^[2], errors crept into the expressions for the density of the internal electromagnetic energy \mathcal{E} and the dielectric tensor ε_{ij} of the crystals MnF_2 , CoF_2 , and NiF_2 . When suitably corrected, formulas (5)–(10) of^[2] become respectively

$$\begin{aligned}
\mathcal{E} &= \mathcal{E}_0 + \frac{1}{8\pi} (\lambda_1 E_x^2 + \lambda_2 (E_x^2 + E_y^2) + \lambda_3 E_z^2 + \lambda_4 (E_x^2 + E_y^2) l_x^2 \\
&\quad + \lambda_5 E_x l_x (E_x l_x + E_y l_y) + \lambda_7 E_x E_y l_x l_y + \lambda_8 (E_x^2 - E_y^2) (l_x^2 - l_y^2)); \\
\varepsilon_{xx} &= \varepsilon_{\perp}^0 + 2\lambda_2 l^2 + 2\lambda_4 l_x^2 + 2\lambda_8 (l_x^2 - l_y^2), \\
\varepsilon_{yy} &= \varepsilon_{\perp}^0 + 2\lambda_2 l^2 + 2\lambda_4 l_x^2 - 2\lambda_8 (l_x^2 - l_y^2),
\end{aligned} \quad (5)$$

$$\begin{aligned}
\varepsilon_{zz} &= \varepsilon_{\parallel}^0 + 2\lambda_1 l^2 + 2\lambda_3 l_z^2, \quad \varepsilon_{xy} = \varepsilon_{yx} = 1/2 \lambda_7 l_x l_y, \\
\varepsilon_{xz} &= \varepsilon_{zx} = 1/2 \lambda_5 l_x l_z, \quad \varepsilon_{yz} = \varepsilon_{zy} = 1/2 \lambda_6 l_y l_z,
\end{aligned} \quad (6)$$

$$\Delta n_{xy}^{\text{isotr.}} = n_x - n_y = l^2 \left(\frac{\lambda_1}{n_{\parallel}^0} - \frac{\lambda_2}{n_{\perp}^0} \right); \quad (7)$$

$$\Delta n_x = n_x - n_y = l^2 \left(\frac{\lambda_1}{n_{||}^0} - \frac{\lambda_2}{n_{\perp}^0} \right) + l_z^2 \left(\frac{\lambda_3}{n_{||}^0} - \frac{\lambda_4}{n_{\perp}^0} \right); \quad (8)$$

$$\Delta n_x^{\text{isotr.}} = n_x - n_y = l^2 \left(\frac{\lambda_1}{n_{||}^0} - \frac{\lambda_2}{n_{\perp}^0} \right) + l_z^2 \left(\frac{\lambda_3}{n_{||}^0} - \frac{\lambda_4}{n_{\perp}^0} \right) + l_x^2 \frac{\lambda_4}{n_{\perp}^0}. \quad (9)$$

$$\Delta n_x = n_x - n_y = \frac{2\lambda_8 l_x^2}{n_{\perp}^0}. \quad (10)$$

In addition, the tensor T_{ij} becomes diagonalized by rotation of the x and z axes through an angle α :

$$\text{tg } 2\alpha = \frac{\lambda_5}{\epsilon_{||}^0 - \epsilon_{\perp}^0} l_x l_z.$$

¹⁾The authors thank N. Yu. Ikornikova, V. R. Gakel', and V. M. Egorov for supplying the MnCO_3 and CoCO_3 samples, and to S. V. Petrov for supplying the CsMnF_3 crystals.

¹⁾A. S. Borovik-Romanov, N. M. Kreĭnes, and M. A. Talalaev, *ZhETF Pis. Red.* **13**, 80 (1971) [*JETP Lett.* **13**, 54 (1971)].

²⁾A. S. Borovik-Romanov, N. M. Kreĭnes, A. A. Pankov, and M. A. Talalaev, *Zh. Eksp. Teor. Fiz.* **64**, 1762 (1973) [*Sov. Phys.-JETP* **37**, 890 (1973)].

³⁾J. F. Dillon, J. P. Remeika, and C. S. Staton, *J. Appl. Phys.*, **40**, 1510 (1969); **41**, 4613 (1970).

⁴⁾R. V. Pisarev, I. G. Siniĭ, and G. A. Smolenskiĭ, *Zh. Eksp. Teor. Fiz.* **57**, 737 (1969) [*Sov. Phys.-JETP* **30**, 404 (1970)].

⁵⁾R. V. Pisarev, I. G. Siniĭ, N. N. Kolpakova, and Yu. M. Yakovlev, *Zh. Eksp. Teor. Fiz.* **60**, 2188 (1971) [*Sov. Phys.-JETP* **33**, 1175 (1971)].

⁶⁾R. V. Pisarev, I. G. Siniĭ, and G. A. Smolenskiĭ, *ZhETF Pis. Red.* **9**, 112, 294 (1969) [*JETP Lett.* **9**, 64, 172 (1969)].

⁷⁾I. G. Siniĭ, R. V. Pisarev, P. P. Syrnikov, G. A. Smolenskiĭ, and A. I. Kapustin, *Fiz. Tverd. Tela* **10**, 2252 (1968) [*Sov. Phys.-Solid State* **10**, 1775 (1969)].

⁸⁾J. R. Jahn and H. Dacks, *Sol. St. Comm.*, **18**, 1617 (1971).

⁹⁾R. A. Alikhanov, *Zh. Eksp. Teor. Fiz.* **37**, 1145 (1959) [*Sov. Phys.-JETP* **10**, 814 (1960)].

¹⁰⁾A. Zalkin, K. Lee, and D. H. Templeton, *J. Chem. Phys.*, **37**, 697 (1962).

¹¹⁾R. A. Alikhanov, *Zh. Eksp. Teor. Fiz.* **39**, 1481 (1960) [*Sov. Phys.-JETP* **12**, 1028 (1961)].

¹²⁾K. Lee, A. M. Portis, and G. L. Witt, *Phys. Rev.*, **132**, 144 (1963).

¹³⁾A. S. Borovik-Romanov, *Zh. Eksp. Teor. Fiz.* **36**, 766 (1959) [*Sov. Phys.-JETP* **9**, 539 (1959)]. A. S. Borovik-Romanov and V. I. Ozhogin, *Zh. Eksp. Teor. Fiz.* **39**, 27 (1960) [*Sov. Phys.-JETP* **12**, 18 (1961)].

¹⁴⁾I. N. Kalinkina, Candidate's dissertation, *Inst. Phys. Prob. USSR Acad. Sci.*, 1962.

¹⁵⁾N. F. Kharchenko, V. V. Eremenko, and O. P. Tutakina, *Zh. Eksp. Teor. Fiz.* **64**, 1326 (1973) [*Sov. Phys.-JETP* **37**, 672 (1973)].

¹⁶⁾A. S. Borovik-Romanov, B. Ya. Kotyuzhanskiĭ, and L. A. Prozorova, *Zh. Eksp. Teor. Fiz.* **58**, 1911 (1970) [*Sov. Phys.-JETP* **31**, 1027 (1970)].

¹⁷⁾J. Kacser, *Zh. Eksp. Teor. Fiz.* **43**, 2042 (1962) [*Sov. Phys.-JETP* **16**, 1443 (1963)].

¹⁸⁾A. Bazhan, *Zh. Eksp. Teor. Fiz.* **65**, 2479 (1973) [*Sov. Phys.-JETP* **38**, 1238 (1974)].

¹⁹⁾R. A. Alikhanov, *J. Phys. Soc. Japan* **17**, Suppl. B-111, 58 (1962).

Translated by J. G. Adashko

87